論文 / 著書情報
Article / Book Information

Title	Dynamic modeling and parameter identification of an elastic rod for analyzing fly-fishing
Authors	Ryousuke Hakamata, Mitsuru Endo, Yusuke Sugahara, Yukio Takeda, Hiroyuki Ishii
Citation	Proceedings of the 5th Jc-IFToMM International Symposium, , , pp. 44-51
Pub. date	2022, 7
DOI	https://doi.org/10.57272/jciftomm.5.0_44
Creative Commons	Information is in the article.

Proceedings of the 5th Jc-IFToMM International Symposium (2022)
The 28th Jc-IFToMM Symposium on Theory of Mechanism and Machines
16th July 2022

Dynamic modeling and parameter identification of an elastic rod for analyzing fly-fishing

RYOUSUKE HAKAMATA, MITSURU ENDO, YUSUKE SUGAHARA, YUKIO TAKEDA
Department of Mechanical Engineering, Tokyo Institute of Technology, Japan,
{hakamata.r.aa, endo.m.au, sugahara.y.ab, takeda.y.aa}@m.titech.ac.jp

HIROYUKI ISHII
Department of Modern Mechanical Engineering, Waseda University, Japan,
hiro.ishii@waseda.jp

ABSTRACT
The authors focus on the fly-fishing to realize a casting by a small and low-power manipulator. This paper proposes a parameter identification method for analyzing real fly-fishing based on a rod dynamic model. First, the static measurement identifies parameters of the rod's elasticity and derives the relationship between the center of gravity and the mass of each link. Then, all parameters are identified through the measurements of rod vibrations by the steepest descent method using a few variables, from approximating each link as a truncated cone. The validity of the proposed method was confirmed by comparing measurements and simulation using identified parameters.
KEY WORDS: Casting, Flexible Link, Fly-fishing, Parameter Identification, Modeling

1. Introduction

In the field of field robotics, expansion of the operating range of a manipulator has been studied. As one of those studies, a manipulator, called a *Casting manipulator* [1], that throws an end-effector attached to the end of a string by using rotational or translational motion has been studied [2][3]. These manipulators can retrieve an object at a distance or move its main body by throwing an end-effector, gripping objects at a distance, and pulling the string. These functions allow manipulators to expand the operating range with a minimal increase in mass.

In the case of expanding the operating range of a small mobile robot, it cannot mount large or heavy objects. When a small casting manipulator throwing a lightweight object or a string as an end-effector can be realized, it can be mounted on a small mobile robot to expand its functions and operating range. When throwing them, aerodynamic force affects behavior of a string significantly due to low mass relative to the surface area. The conventional methods utilizing the mass of the end-effector are not suitable for that throwing. The reason for this is that they require high power outputs and a larger device when extending target distance of throwing a lightweight object. In order for a small mobile robot to perform the above functions, the manipulator needs to be able to throw a lightweight object with low-power even if the target throwing distance is extended.

Here, fly-fishing, a kind of fishing method, is thought to be one throwing method to solve this problem. The method does not utilize the mass mounted on the flexible string's tip, such as a lure or a sinker of other fishing methods, but utilizes the elasticity of the rod and the mass of the flexible string itself [4], which is released from the rod's tip [5]. This flexible string is called a "line". Among the various fly-casting methods, the false cast is the most typical and the furthest casting method. The method consists of the forward cast and the back cast [6]. The forward cast is the way to cast the line to the front side of the fisherman by swinging the rod forward (Fig. 1a). The back cast is the opposite of the forward cast (Fig. 1b). The false cast is realized when the fisherman performs the forward cast and the back cast repeatedly. The line is restrained by gripping near the rod's base, and it extends out from the rod's tip for an appropriate length. It is known that a U-shaped loop of the line will be

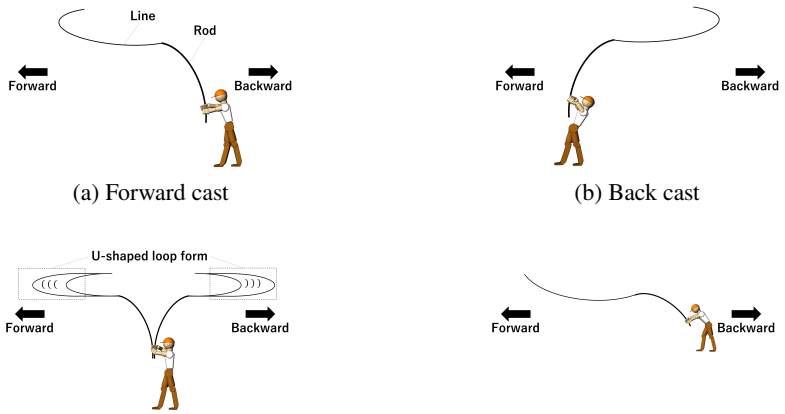

(a) Forward cast (b) Back cast

(c) Loop creation (d) Swing downward of a rod

Fig. 1 Motion of fly-fishing

formed by switching the forward cast and the back cast at the moment when the line is fully extended [7] (Fig. 1c). The line is released from the rod's tip due to the inertial force of the line during the forward cast. The loop of the line expands gradually when the line is released sequentially for an appropriate time. After the loop shape is long enough, the rod is swung down, the loop shape extends, and the line flies to the target point (Fig. 1d). A characteristic of fly-fishing is that when the target casting distance is far, the fisherman is simply required to continue the slow, repetitive motion for a longer duration. This study aims to realize the casting of a flexible string with a small and low-power manipulator based on the principle of fly-fishing.

Some dynamic simulation methods of fly-fishing were proposed. Watanabe *et al.* [5], for example, proposed a numerical simulation method by modeling the rod and the line as a serial chain composed of multiple links. Various real fly-fishings are simulated by this method [8][9]. In addition, a method proposed by the authors [10] models the line as multiple links whose length are variable according to the line's sequential release. However, there are no studies that consider repetitive motion, which is one of the important procedures of fly-fishing for long casting distance. In particular, no method has been established for forming the desired line shape in the air through repetitive motion.

This study aims to apply the principle to a manipulator through analyzing the periodic motion of real fly-fishing. In this paper, the method of parameter identification of the rod as a serial chain composed of multiple links is proposed for the analysis. Here, the mass, the center of gravity (CoG), and the moment of inertia of each link of the rod, and the rotational spring coefficient and damping coefficient of each joint are targets for identification. First, the static measurements are used to identify rotational spring coefficients. Then, the measurements of rod vibrations are used to identify other parameters by the steepest descent method. The validity of the proposed method was confirmed by the identification using motion capture measurements. Also, the possibility that the rotational spring coefficients are not constant is indicated by comparing the identification results for three different time-ranges in a same vibration.

2. Dynamic modeling of rod

The rod and the line are modeled as a planar chain consisting of multiple rigid elements jointed by revolute joints with rotational springs and dampers as shown in Figs. 2 and 3. The parameters used

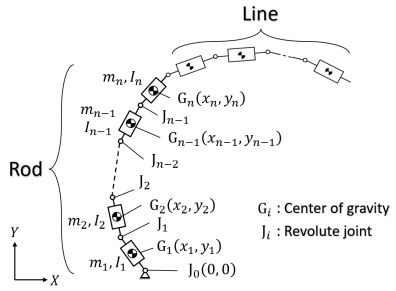

Fig. 2 Rod and line as a serial chain composed of multiple links

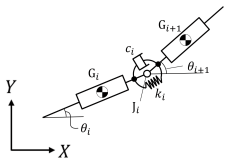

Fig. 3 Joint between links

here are defined as follows.

c_i : Rotational damping coefficient	$\boldsymbol{M} = [m_1,\ m_2,\ \cdots,\ m_n]$	: Mass vector
g : Gravitational acceleration	$\boldsymbol{M_r} = \mathrm{diag}[m_1\ m_1\ m_2\ m_2\ \cdots\ m_n\ m_n]$	: Mass matrix
i : Link number $(1 \sim n)$	$\boldsymbol{M_\phi} = \mathrm{diag}[I_1\ I_2\ \cdots\ I_n]$	: Inertia tensor
I_i : Inertia of link	$\boldsymbol{r} = [x_1,\ y_1,\ \cdots,\ x_n,\ y_n]$	: Position vector
k_i : Rotational spring coefficient	$\boldsymbol{\phi} = [\theta_1,\ \theta_2,\ \cdots,\ \theta_n]$	: Orientation angle vector
l_i^L : $\overline{\mathrm{J}_i\mathrm{G}_i}$	$\boldsymbol{q} = [\boldsymbol{r}^T,\ \boldsymbol{\phi}^T]$	: Generalized coordinate vector
l_i^R : $\overline{\mathrm{G}_i\mathrm{J}_{i-1}}$	$\boldsymbol{Q} = [\boldsymbol{Q_r}^T,\ \boldsymbol{Q_\phi}^T]$	: Gereralized force
l_i : $l_i^R + l_i^L$		
m_i : Mass of link		
τ : Torque applied to rod's base		

Here, $\boldsymbol{Q_r} \in \mathbb{R}^{2n}$ and $\boldsymbol{Q_\phi} \in \mathbb{R}^n$ are defined as follows, respectively.

$$\boldsymbol{Q_r} = [0,\ -m_1 g,\ 0,\ -m_2 g,\ \cdots,\ 0,\ -m_n g] \tag{1}$$

$$\boldsymbol{Q_{\phi i}} = \begin{cases} \tau + k_1(\theta_2 - \theta_1) + c_1(\dot{\theta}_2 - \dot{\theta}_1) & \text{if} \quad i = 1 \\ -k_{n-1}(\theta_n - \theta_{n-1}) - c_{n-1}(\dot{\theta}_n - \dot{\theta}_{n-1}) & \text{if} \quad i = n \\ -k_{i-1}(\theta_i - \theta_{i-1}) - c_{i-1}(\dot{\theta}_i - \dot{\theta}_{i-1}) + k_i(\theta_{i+1} - \theta_i) + c_i(\dot{\theta}_{i+1} - \dot{\theta}_i) & \text{otherwise.} \end{cases} \tag{2}$$

In the previous study [5], the rod was modeled with the Lagrange multipliers method by Eq. (3).

$$\begin{bmatrix} \boldsymbol{M_r} & 0 & \boldsymbol{\Phi_r}^T \\ 0 & \boldsymbol{M_\phi} & \boldsymbol{\Phi_\phi}^T \\ \boldsymbol{\Phi_r} & \boldsymbol{\Phi_\phi} & 0 \end{bmatrix} \begin{bmatrix} \ddot{\boldsymbol{r}} \\ \ddot{\boldsymbol{\phi}} \\ \boldsymbol{\lambda} \end{bmatrix} = \begin{bmatrix} \boldsymbol{Q_r} \\ \boldsymbol{Q_\phi} \\ \boldsymbol{\gamma} \end{bmatrix} \tag{3}$$

Here, $\boldsymbol{\lambda} \in \mathbb{R}^{2n}$ is the Lagrange multiplier vector, $\boldsymbol{\Phi} \in \mathbb{R}^{2n}$ is constraint equations derived from the geometric relationship of each link as follows. $\boldsymbol{\Phi_r}$ and $\boldsymbol{\Phi_\phi}$ are partial derivatives of $\boldsymbol{\Phi}$ with respect to $\boldsymbol{r}$ and $\boldsymbol{\phi}$, respectively. $\boldsymbol{\gamma} \in \mathbb{R}^{2n}$ is a vector that can be derived as follows.

$$\boldsymbol{\Phi}_1 = \begin{bmatrix} l_1^L \cos\theta_1 - x_1 \\ l_1^L \sin\theta_1 - y_1 \end{bmatrix} \tag{4}$$

$$\boldsymbol{\Phi}_i = \begin{bmatrix} x_{i-1} + l_i^R \cos\theta_{i-1} + l_i^L \cos\theta_i - x_i \\ y_{i-1} + l_i^R \sin\theta_{i-1} + l_i^L \sin\theta_i - y_i \end{bmatrix} \quad (2 \le i \le n) \tag{5}$$

$$\boldsymbol{\Phi} = \begin{bmatrix} \boldsymbol{\Phi}_1^T & \boldsymbol{\Phi}_2^T & \cdots & \boldsymbol{\Phi}_n^T \end{bmatrix}^T = \boldsymbol{0} \tag{6}$$

$$\boldsymbol{\gamma} = -\frac{\partial}{\partial \boldsymbol{q}} \left(\frac{\partial \boldsymbol{\Phi}}{\partial \boldsymbol{q}} \dot{\boldsymbol{q}} \right) \dot{\boldsymbol{q}} \tag{7}$$

The following equations of motion for ϕ are derived by solving Eq. (3). The behavior of the rod is calculated under a given torque applied at the rod's base or the behavior of the first link.

$$\left\{ \boldsymbol{M_\phi} + \boldsymbol{\Phi_\phi}^T \left(\boldsymbol{\Phi_r}^T \right)^{-1} \boldsymbol{M_r} \boldsymbol{\Phi_r}^{-1} \boldsymbol{\Phi_\phi} \right\} \ddot{\boldsymbol{\phi}} = \boldsymbol{Q_\phi} - \boldsymbol{\Phi_\phi}^T \left(\boldsymbol{\Phi_r}^T \right)^{-1} \left(\boldsymbol{Q_r} - \boldsymbol{M_r} \boldsymbol{\Phi_r}^{-1} \boldsymbol{\gamma} \right) \tag{8}$$

3. Identification method

3.1 Identification parameters

Among the parameters, the number of links n is predetermined. The length of each link l_i and the overall mass $m_{total} = \sum_{i=1}^{n} m_i$ are measurable parameters. The parameters CoG, the mass, and the moment of inertia of each link are difficult to measure. These parameters affect the period of a rod vibration. Although the rotational spring coefficients can be obtained from the material properties and link lengths [5], it is difficult to derive them for actual "unconstant" rod. In this paper, "unconstant" means that the cross-sectional shape and materials are not uniform. It is considered more effective to obtain them from measurements of an actual rod motion.

On the other hand, the rotational damping coefficients have been assumed in [5] to be all equal and small enough because it is impossible to calculate. In other studies, the rotational damping coefficients are manually adjusted so that the result of the simulations and measurements agreed well [11]. In fly-fishing, the periodic motion of the rod changes gradually, and it is difficult to manually adjust the parameters to match simulation results and every periodic motions.

Therefore, in this paper, $m_i, I_i, k_i, c_i, l_i^L$ are target parameters for identification.

3.2 Identification method based on static measurements

First, the rotational spring coefficients are identified. For this process, balanced conditions with weights attached to the joints are observed. Assume the base is similar to other joints where the torque at the base is expressed by a rotational spring, as shown in Eq. (9). This assumption is the same as in Section 2, where the rod is divided into $n+1$ links and n links other than the first link are considered. For simplicity, link numbers are from 0 to n.

$$\tau = -k_0(\theta_1 - \theta_0) \tag{9}$$

The mass of the weight attached to J_i is defined as m_{wi} and let $\boldsymbol{M}_w = [m_{w1},\ m_{w2},\ \cdots,\ m_{wn}]$. When the rod is fixed at the base in the static state, Eq. (10) is held by Eq. (8). $\boldsymbol{\Phi}'_{\boldsymbol{y}}$ and $\boldsymbol{\Phi}'_{\boldsymbol{\phi}}$ are partial derivatives of $\boldsymbol{\Phi}' \in \mathbb{R}^n$ with respect to $\boldsymbol{y} = [y_1,\ y_2,\ \cdots,\ y_n]$ and $\boldsymbol{\phi}$, respectively.

$$\boldsymbol{Q}_\phi - \boldsymbol{C}_\phi \boldsymbol{L}_R \boldsymbol{M}_w g = -\boldsymbol{\Phi}'^T_{\boldsymbol{\phi}} \left(\boldsymbol{\Phi}'^T_{\boldsymbol{y}}\right)^{-1} (\boldsymbol{M} + \boldsymbol{M}_w)\, g \tag{10}$$

$$\boldsymbol{C}_\phi = \mathrm{diag}[\cos\theta_1\ \cos\theta_2\ \cdots\ \cos\theta_n] \tag{11}$$

$$\boldsymbol{L}_R = \mathrm{diag}[l_1^R\ l_2^R\ \cdots\ l_n^R] \tag{12}$$

$$\boldsymbol{\Phi}'_i = y_{i-1} + l_1^R \sin\theta_{i-1} + l_1^L \sin\theta_i - y_i \tag{13}$$

Here, Eq. (10) is expressed from Eq. (1) and Eq. (2) as follows.

$$\boldsymbol{\Theta}\boldsymbol{K} = \boldsymbol{C}_\phi \left\{ (\boldsymbol{L}_L + \boldsymbol{L}_z)\, \boldsymbol{M} + (\boldsymbol{L} + \boldsymbol{L}_z)\, \boldsymbol{M}_w \right\} g \tag{14}$$

$$\boldsymbol{\Theta}_{ij} = \begin{cases} \theta_i - \theta_{i+1} & \text{if} \quad i = j \\ \theta_{i+2} - \theta_{i+1} & \text{if} \quad i+1 = j \\ 0 & \text{otherwise.} \end{cases} \tag{15}$$

$$\boldsymbol{K} = [k_0,\ k_1,\ \cdots,\ k_{n-1}] \tag{16}$$

$$\boldsymbol{L}_L = \mathrm{diag}[l_1^L\ l_2^L\ \cdots\ l_n^L] \tag{17}$$

$$\boldsymbol{L}_{zij} = \begin{cases} l_i & \text{if } i < j \\ 0 & \text{otherwise.} \end{cases} \tag{18}$$

$$\boldsymbol{L} = \mathrm{diag}[l_1\ l_2\ \cdots\ l_n] \tag{19}$$

$\boldsymbol{\Theta}$ and $\boldsymbol{C}_\phi$ are matrices derived from the static measurement, while $\boldsymbol{L}_z$, $\boldsymbol{L}$, and $\boldsymbol{M}_w$ are matrices or vectors measured in advance. From the above, $\boldsymbol{K}$ and $(\boldsymbol{L}_L + \boldsymbol{L}_z)\, \boldsymbol{M}$ can be derived once the balanced conditions for at least two types of load application are observed, including the no-load condition. If no weight is attached to the rod's tip in all measurements, $\boldsymbol{K}$ cannot be derived because

$\boldsymbol{C}_{\phi a}^{-1}\boldsymbol{\Theta}_a - \boldsymbol{C}_{\phi b}^{-1}\boldsymbol{\Theta}_b$ is no longer theoretically regular. Therefore, measurement with a weight attached to the tip of the rod is essential. Here, one of the two types of measurements is subscripted a, and the other is subscripted b.

$$\boldsymbol{K} = \left(\boldsymbol{C}_{\phi a}^{-1}\boldsymbol{\Theta}_a - \boldsymbol{C}_{\phi b}^{-1}\boldsymbol{\Theta}_b\right)^{-1} (\boldsymbol{L} + \boldsymbol{L}_z)\,(\boldsymbol{M}_{wa} - \boldsymbol{M}_{wb})g \tag{20}$$

$$(\boldsymbol{L}_L + \boldsymbol{L}_z)\,\boldsymbol{M} = \frac{1}{g}\boldsymbol{C}_{\phi a}^{-1}\boldsymbol{\Theta}_a\boldsymbol{K} - (\boldsymbol{L} + \boldsymbol{L}_z)\,\boldsymbol{M}_{wa} \tag{21}$$

This equations mean that $\boldsymbol{K}$ and $(\boldsymbol{L}_L + \boldsymbol{L}_z)\,\boldsymbol{M}$ can be identified and derived respectively from static measurements.

3.3 Identification method based on rod vibration

3.3.1 Approximation of inertia moment of links

In this section, I_i is approximated by considering each link as a truncated cone. This approximation makes it possible to obtain the mass and moment of inertia from the position of the CoG using the previous section's method and to reduce the number of parameters to be identified.

The i^{th} link is considered as a truncated cone of radius R_{i1} on the top surface, radius R_{i2} on the bottom surface, height $l_i (>> R_{i1}, R_{i2})$, and density ρ_i. Let $r_{iR} = R_{i1}/R_{i2}$ and $r_{il} = l_i^L/l_i$, then r_{iR} can be obtained from using r_{il} as follows. Here, r_{il} should be in $0.25 \leq r_{il} \leq 0.75$. Then, I_i is approximated as follows.

$$r_{iR} = \frac{2r_{il} - 1 + \sqrt{-12r_{il}^2 + 12r_{il} - 2}}{3 - 4r_{il}} \tag{22}$$

$$I_i \approx \frac{3}{80} m_i l_i^2 \frac{(1 + r_{iR})^4 + 4r_{iR}^2}{\left(1 + r_{iR} + r_{iR}^2\right)^2} \tag{23}$$

3.3.2 Identification procedure using steepest descent method

In the dynamic model of a rod, assume the base is similar to other joints where the torque at the base is expressed by a rotational spring and a rotational damper, as shown in Eq. (24).

$$\tau = -k_0(\theta_1 - \theta_0) - c_0(\dot{\theta}_1 - \dot{\theta}_0) \tag{24}$$

From the previous sections, m_i, l_i^L and I_i are derived when r_{li} is determined. Therefore, the steepest descent method is applied to r_{li} and c_i. Here, assume that the value of c_i is r_{ci} times k_i. The evaluation function E is defined as follows.

$$E = \int_0^T (\boldsymbol{\phi}_A(t) - \boldsymbol{\phi}_S(t))^T\,(\boldsymbol{\phi}_A(t) - \boldsymbol{\phi}_S(t))\,dt \tag{25}$$

Where, T is a long enough measurement time, $\boldsymbol{\phi}_A$ is the actual angle obtained by measurement, $\boldsymbol{\phi}_S$ is the angle obtained by simulation. The updated equation of $\boldsymbol{r}_l = [r_{l1},\ r_{l2},\ \cdots,\ r_{ln}]$ and $\boldsymbol{r}_c = [r_{c0},\ r_{c1},\ \cdots,\ r_{cn-1}]$ is shown below. Here, α_l and α_c are learning rates.

$$r_{li}^{(k+1)} = r_{li}^{(k)} - \alpha_l \left(\frac{\partial E}{\partial r_{li}}\right)^{(k)} \tag{26}$$

$$r_{ci}^{(k+1)} = r_{ci}^{(k)} - \alpha_c \left(\frac{\partial E}{\partial r_{ci}}\right)^{(k)} \tag{27}$$

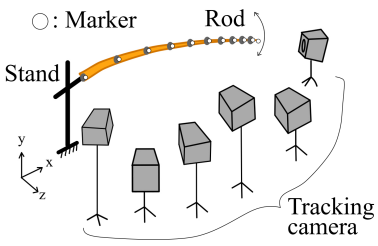

Fig. 4 Measurement overview

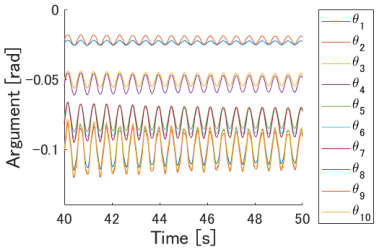

Fig. 5 Measurement result

Table 1 Identified values

k_i [N·m/rad]	l_i^L [mm]	m_i [g]
k_0 : 24.3	l_1^L: 373	m_0: 37.7
k_1 : 7.93	l_2^L: 270	m_1: 28.8
k_2 : 3.23	l_3^L: 285	m_2: 12.5
k_3 : 0.631	l_4^L: 210	m_3: 11.5
		m_4: 6.5

l_i^L and m_i are identified by repeating this update until the following equation is satisfied. Here, $\delta(> 1)$ is a threshold value and the mass of the 0-th link can be derived by $m_0 = m_{total} - \sum_{i=1}^{n} m_i$.

$$1 \leq \frac{E^{(k)}}{E^{(k+1)}} < \delta \tag{28}$$

When the identification time-range is long enough, large errors are expected at some times. This is because c_i is possibly not a constant. In this paper, the variation of c_i is analyzed by the identification of c_i for short time-ranges. The steepest descent method is applied to $\boldsymbol{r}_c$ in the same way after the identification of the others.

4. Numerical example and discussion

4.1 Determination of number of links

The overview of experiment setup is shown in Fig. 4. The rod used for identification was LOCHMOP F865-4 weighing 97 g made by DAIWA. OptiTrack Flex 13 was used for motion capture, and measurements were taken at 120 Hz. Also, Motive and VENUS3D R were used for control and analysis, respectively. The markers were attached based on the 11 guides, which are the holes through which the line is to be passed on the rod. First, the rod was fixed to a stand that allowed the attachment angle at the base to be varied. In order to determine the number of links, the base was fixed at various angles and the free vibration were measured. Next, a 50 g weight was suspended from the rod's tip to sufficiently bend the rod, and it was detached to vibrate the rod on a plane as much as possible. The low-pass filter with 15 Hz cutoff frequency is applied to the measurement data based on the result of the Fourier transform.

One experiment of the measurement results is shown in Fig. 5. There are four different convergence angles for the ten links. When the convergence angles are approximately equal, the front and rear links are nearly rigid and sensitive to measurement error. Therefore, each set of links is considered as one link. As a result, the number of links n was determined to be four. The link lengths were $l_0 = 261$ mm, $l_1 = 760$ mm, $l_2 = 559$ mm, $l_3 = 623$ mm, $l_4 = 388$ mm.

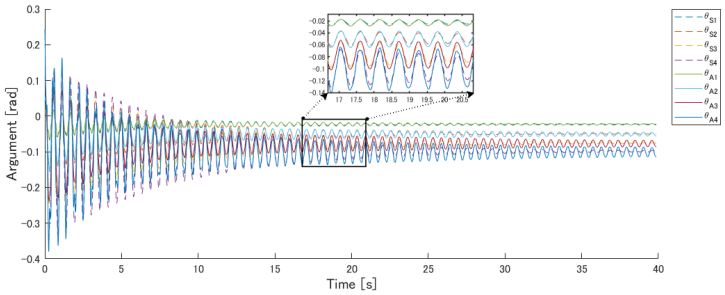

Fig. 6 Simulation and measurements of rotational angle of the each link for a long time-ranges

Table 2 Identified values of rotational damping coefficients

Identification time-range	c_i [N·m·s/rad]				E [m^2]
	c_0	c_1	c_2	c_3	
0 s$\leq t \leq$40 s	4.91×10^{-2}	1.60×10^{-2}	5.43×10^{-3}	7.31×10^{-4}	5.14×10^{-4}
0 s$\leq t \leq$3 s	6.16×10^{-2}	2.85×10^{-2}	5.23×10^{-3}	2.15×10^{-4}	4.68×10^{-4}
20 s$\leq t \leq$23 s	1.80×10^{-2}	1.52×10^{-2}	5.25×10^{-3}	8.08×10^{-4}	1.32×10^{-5}

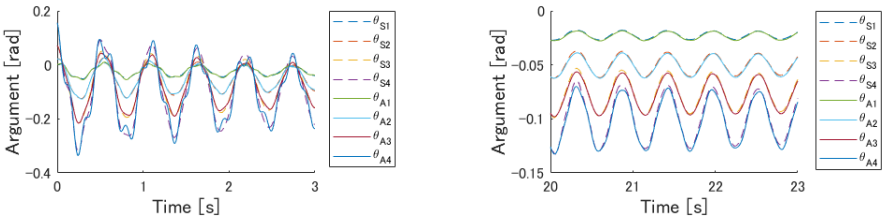

(a) Time-range : 0 s$\leq t \leq$3 s (b) Time-range : 20 s$\leq t \leq$23 s

Fig. 7 Simulation and measurements of rotational angle of the each link for short time-ranges

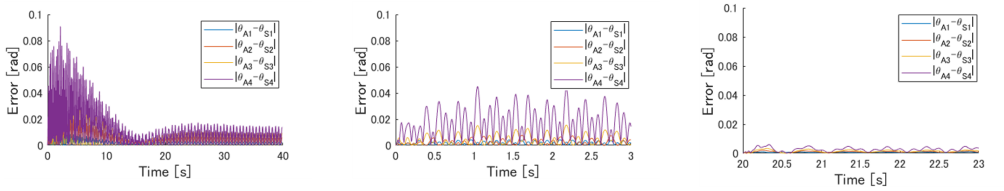

(a) Time-range : 0 s$\leq t \leq$40 s (b) Time-range : 0 s$\leq t \leq$3 s (c) Time-range : 20 s$\leq t \leq$23 s

Fig. 8 Error between simulation and measurements

4.2 Result based on static measurements

The static conditions to be observed were no load and a 100 g weight attached to the rod's tip. The identified parameters k_i are shown in Table 1. This result indicates that the elasticity of the joint decreases as it gets closer to the rod's tip.

4.3 Result based on measurements of rod vibrations

The initial position was defined as a state with a sufficient displacement. The initial conditions for $\boldsymbol{r}_l$ was 0.5 for all elements due to the estimation that the CoG is near the center of the link. The initial

condition for $\boldsymbol{r}_c$ was set to 10^{-5}. The threshold δ were set to 1.001. The identified l_i^L and m_i are shown in Table 1. The simulated and actual behavior of rotational angle of the rod are shown in Fig. 6. This indicates that the period of the rod vibration appears to be well reproduced, and the elasticity of the rod and the moment of inertia of each link are identified with a good accuracy. The above results confirm that the proposed method is effective for identifying parameters of a dynamic model of a rod.

c_i identified for the three time-ranges are shown in Table 2. This indicates that c_i differs depending on the joints. Also, c_i varies greatly depending on the time-range to be identified. This indicates that c_i is not a constant. The behavior simulated by using identified parameters is shown in Fig. 7 for each identification time-range. Also, the error between simulation and measurements before and after the identification of c_i is shown in Fig. 8 for each identification time-range. The above results confirm that the proposed method for identifying rotational damping coefficients in a short time. The identification result for a long time-range has a wide scatter in error, while the identification results for short time-ranges have smaller errors.

Therefore, it seems that considering c_i as a function with respect to the angular velocity or the amplitude of the rod vibration is effective for the rod vibration. This will be investigated in the future work.

5. Conclusion

This paper proposes a parameter identification method for a dynamic model of a flexible rod to analyze fly-fishing. The rod is modeled as a serial chain composed of multiple links. In this paper, the mass, the center of gravity (CoG), and the moment of inertia of each link, and the rotational spring coefficient and damping coefficient of each joint are targets for identification. The summary is as follows.

(1) A method to identify the elasticity of the rod and to derive equations for the mass and the CoG of each link by static state of the rod was proposed.
(2) Moment of inertia of each link was approximated by considering it as a truncated cone in order to reduce the number of parameters to be identified.
(3) Parameters were identified based on measurements of rod vibrations for a long time and short times by the steepest descent method.
(4) The parameters of the actual rods were identified based on static measurements and measurements of rod vibrations, and the effectiveness of the proposed method in identifying parameters for a dynamic model of a rod in a short time period is confirmed.

REFERENCES

[1] H. Arisumi, T. Kotoku, and K. Komoriya. A study of casting manipulation (swing motion control and planning of throwing motion). In *Proc. IEEE/RSJ IROS*, Vol. 1, pp. 168–174, 1997.
[2] H. Arisumi, M. Otsuki, and S. Nishida. Launching penetrator by casting manipulator system. In *IEEE/RSJ IROS*, pp. 5052–5058, 2012.
[3] H. Tsukagoshi, E. Watari, K. Fuchigami, and A. Kitagawa. Casting device for search and rescue aiming higher and faster access in disaster site. In *IEEE/RSJ IROS*, pp. 4348–4353, 2012.
[4] C. Gatti-Bono and N. PERKINS. Physical and numerical modelling of the dynamic behavior of a fly line. *JSV*, Vol. 255, pp. 407–414, 2002.
[5] T. Watanabe and K. Tanaka. Dynamics of a fly line (modeling and analysis). *Trans. JSME, Ser.C*, Vol. 69, No. 680, pp. 1065–1071, 2003.
[6] T. Watanabe and K. Tanaka. Dynamics of a fly line (false cast). *Transe. JSPE*, Vol. 75, No. 12, pp. 1464–1469, 2009.
[7] G. A. Spolek. The mechanics of flycasting: The flyline. *AJP*, Vol. 54, No. 9, pp. 832–836, 1986.
[8] T. Watanabe. Dynamics of a fly line (double haul cast). *Trans. JSME, Ser. C*, Vol. 74, No. 740, pp. 798–805, 2008.
[9] T. Watanabe and A. Tomoda. Dynamics of a fly line (roll cast). *Transe. JSPE*, Vol. 79, No. 1, pp. 104–111, 2013.
[10] R. Hakamata, M. Endo, Y. Sugahara, H. Ishi, and Y. Takeda. Study on casting by using compact and low-power manipulator based on the principle of fly-fishing - 1st report: Modeling of line with consideration of releasing from rod -. In *Proc. of JSME Robomech*, Vol. 2021, pp. 2P3–H15, 2021.
[11] S. Yamabe, S. Nishioka, A. Terayama, and K. Hiromitsu. Analysis of rod-tip response to fish bite by multi-link model. *Transe. JSPE*, Vol. 76, No. 7, pp. 827–833, 2010.